J. Neurovirol. (2012) 18:172–180
DOI 10.1007/s13365-012-0095-0

Immunohistochemical detection of intra-neuronal VZV proteins in snap-frozen human ganglia is confounded by antibodies directed against blood group A1-associated antigens

Werner J. D. Ouwendijk · Sarah E. Flowerdew · Desiree Wick · Anja K. E. Horn · Inga Sinicina · Michael Strupp · Albert D. M. E. Osterhaus · Georges M. G. M. Verjans · Katharina Hüfner

Received: 20 February 2012 / Revised: 15 March 2012 / Accepted: 21 March 2012 / Published online: 28 April 2012

Abstract Varicella-zoster virus (VZV) causes chickenpox, establishes latency in trigeminal (TG) and dorsal root ganglia (DRG), and can lead to herpes zoster upon reactivation. The VZV proteome expressed during latency remains ill-defined, and previous studies have shown discordant data on the spectrum and expression pattern of VZV proteins and transcripts in latently infected human ganglia. Recently, Zerboni and colleagues have provided new insight into this discrepancy (Zerboni et al. in J Virol 86:578–583, 2012). They showed that VZV-specific ascites-derived monoclonal antibody (mAb) preparations contain endogenous antibodies directed against blood group A1 proteins, resulting in false-positive intra-neuronal VZV staining in formalin-fixed human DRG. The aim of the present study was to confirm and extend this phenomenon to snap-frozen TG (n=30) and DRG (n=9) specimens of blood group genotyped donors (n=30). The number of immunohistochemically stained neurons was higher with mAb directed to immediate early protein 62 (IE62) compared with IE63. The IE63 mAb-positive neurons always co-stained for IE62 but not vice versa. The mAb staining was confined to distinct large intra-neuronal vacuoles and restricted to $A1^{POS}$ donors. Anti-VZV mAb staining in neurons, but not in VZV-infected cell monolayers, was obliterated after mAb adsorption against blood group A1 erythrocytes. The data presented demonstrate that neuronal VZV protein expression detected by ascites-derived mAb in snap-frozen TG and DRG of blood group $A1^{POS}$ donors can be misinterpreted due to the presence of endogenous antibodies directed against blood group A1-associated antigens present in ascites-derived VZV-specific mAb preparations.

Keywords Varicella-zoster virus · Snap-frozen human sensory ganglia · Ascites-derived monoclonal antibodies · Immunohistochemistry · False-positive · ABO genotype A1

Werner J. D. Ouwendijk and Sarah E. Flowerdew contributed equally to the manuscript.

W. J. D. Ouwendijk · A. D. M. E. Osterhaus · G. M. G. M. Verjans
Department of Virology, Erasmus Medical Center,
Rotterdam, The Netherlands

S. E. Flowerdew · D. Wick · M. Strupp · K. Hüfner (✉)
Department of Neurology, Ludwig-Maximilians University,
Marchioninistr. 23,
81377 Munich, Germany
e-mail: katharina.huefner@med.uni-muenchen.de

S. E. Flowerdew · D. Wick · A. K. E. Horn · M. Strupp · K. Hüfner
Integrated Research and Treatment Center for Vertigo IFB^{LMU},
Ludwig-Maximilians University,
Munich, Germany

A. K. E. Horn
Institute of Anatomy, Department I,
Ludwig-Maximilians University,
Munich, Germany

I. Sinicina
Department of Legal Medicine, Ludwig-Maximilians University,
Munich, Germany

Introduction

Varicella-zoster virus (VZV) is an endemic human alpha herpesvirus that is typically acquired in early childhood

and is the causative agent of chickenpox (Arvin 1996). After primary infection, the virus establishes a lifelong latent infection of sensory neurons of the trigeminal ganglia (TG) and dorsal root ganglia (DRG). In about one in five latently infected individuals, the virus reactivates later in life to cause herpes zoster (shingles), a number that can be approximately halved by VZV vaccination of adults (Mick 2010; Oxman et al. 2005). Individuals with declining VZV-specific cellular immunity, including immunocompromised patients and the elderly, are at risk of developing herpes zoster. Factors such as the host restriction of VZV and the difficulty in obtaining high titers of cell-free virus have hindered advances in elucidating the virus and host factors involved in VZV latency and reactivation in humans.

DNA polymerase chain reaction (PCR) analysis has long been used to identify virus-specific nucleic acids in human sensory ganglia, with VZV DNA present in about 90 % of TG and slightly fewer DRG (Inoue et al. 2010; Mahalingam et al. 1992). The frequency of individual VZV-positive neurons has been determined at about 4.1 % (Wang et al. 2005). The exact composition of the VZV latency-associated transcriptome and proteome is still a matter of debate. The VZV genome encompasses 68 unique open reading frames (ORF), which are coordinately expressed during lytic infection. In contrast to latent herpes simplex virus infections, in which predominantly the non-coding latency-associated transcript and no viral protein is detectable (Croen et al. 1987; Stevens et al. 1987), transcripts of the VZV genes 21, 29, 62, 63, and 66 have been consistently detected in latently infected human sensory ganglia using a wide array of molecular biology techniques such as Northern Blot (Meier et al. 1993), in situ hybridization (Kennedy et al. 2000), PCR analysis of cDNA libraries (Cohrs et al. 1994, 1996), reverse transcriptase-polymerase chain reaction (RT-PCR), and quantitative RT-PCR (Cohrs and Gilden 2007), as well as multiplex RT-PCR and the GeXPS System (Nagel et al. 2011). Transcripts of the VZV genes 4 and 18 have only incidentally been reported (Kennedy et al. 1999, 2000). Recently, Nagel and colleagues have used multiplex RT-PCR to determine the entire VZV transcriptome in latently VZV-infected human TG, reporting on the transcription of additional VZV genes including 11, 41, 43, 57, and 68 (Nagel et al. 2011).

The VZV latency-associated proteome is even more enigmatic, having only been studied using immunohistochemistry (IHC), and with discordant results on the expression of viral proteins compared with their corresponding transcripts (Cohrs et al. 2003; Grinfeld and Kennedy 2004; Kennedy et al. 2000; Lungu et al. 1998; Mahalingam et al. 1996; Zerboni et al. 2010). Also, a higher frequency of neurons was found positive for VZV protein compared with VZV DNA (Wang et al. 2005). Proteins encoded by VZV ORF 4, 21, 29, 62, 63, and 66 have been detected in the cytoplasm of ganglionic neurons with variable results depending on the antibody format (rabbit polyclonal and mouse monoclonal antibodies (mAb)), the antibody source (mAb clones), and the tissues examined (DRG and TG being either formalin-fixed or snap-frozen) (Cohrs and Gilden 2003; Grinfeld and Kennedy 2004; Kennedy et al. 2000; Lungu et al. 1998; Mahalingam et al. 1996; Theil et al. 2003; Zerboni et al. 2010). The expression of the immediate early proteins 62 (IE62) and IE63 has been most widely studied. The frequency of IE62- and IE63-expressing neurons varied extensively between studies ranging from incidental positive neurons to about one in four neurons positive in human ganglia (Cohrs and Gilden 2003; Grinfeld and Kennedy 2004; Kennedy et al. 2000; Lungu et al. 1998; Mahalingam et al. 1996; Theil et al. 2003; Zerboni et al. 2010).

Recently, Zerboni and colleagues have provided new insight into the described discrepancies (Zerboni et al. 2012). They showed that VZV-specific ascites-derived mAb and rabbit antibody preparations, but not tissue culture-derived VZV mAb, contain endogenous anti-human blood group A1 antibodies. Among other cells, sensory neurons express blood group A1-associated antigens within cytoplasmic vacuoles that are part of the Golgi apparatus (Dodd and Jessell 1985; Mollicone et al. 1986) resulting in false-positive intra-neuronal VZV staining in formalin-fixed latently VZV-infected human DRG (Zerboni et al. 2012). This aberrant staining pattern could be attributed to the formalin fixation exposing the respective blood group antigenic epitopes for antibody recognition. The aim of the present study was to confirm and extend this aberrant VZV protein immunohistology finding to snap-frozen TG and DRG specimens of blood group genotyped donors.

Materials and methods

Human tissue samples and preparation of VZV-infected cells

The current study was performed on 39 human sensory ganglia comprising 30 TG from 25 donors and nine DRG from seven donors (Table 1). The average age of the donors was 63.0±4 years (±SEM), and the average post-mortem delay was 13.8±1.8 h. Fifteen TG and nine DRG were autopsy samples obtained at the Ludwig-Maximilians University (Munich, Germany), and the use thereof was approved by the Ethics Committee of the Medical Faculty of the Ludwig-Maximilians University in Munich. An additional 15 TG were obtained from The Netherlands Brain Bank (NBB) at the Netherlands Institute for Neuroscience (Amsterdam, The Netherlands). All NBB-derived tissues have been collected from donors from whom a written

Table 1 Donor blood type and VZV protein immunohistochemistry results on human sensory ganglia assayed

Nr	Ganglion type	Age (years); sex	Diagnosis at death	Anti-VZV mAb		ABO genotype	ABO phenotype
				IE62	IE63		
1	TG	93; F	Non-demented/Lewy bodies	+	+	A101-B101	A1B
2	TG	87; F	Parkinson	+	+	A101-A101	A1
3	TG	52; M	Pick's disease	–	–	A201-O01	A2
4	TG	73; F	Alzheimer, Lewy bodies	+	–	A101-A101	A1
5	TG	84; F	Alzheimer	+	+	A101-O01	A1
6	TG	51; M	Pick's disease	–	–	A101-A201	A1A2
7	TG	70; M	Pick's disease	–	–	A201-A201	A2
8	TG	67; M	Parkinson	+	–	A101-A201	A1A2
9	TG	81; F	Alzheimer	+	+	A101-B101	A1B
10	TG	70; M	Alzheimer	–	–	O01-O01	O
11	TG	68; F	Pick's disease	–	–	O01-O01	O
12	TG	41; F	Pick's disease	–	–	A101-A201	A1A2
13	TG	77; M	Parkinson	–	–	A101-O03	A1
14	TG	93; F	Non-demented control	–	–	O01-O01	O
15	TG	77; F	Alzheimer	–	–	O01-O01	O
16	TG	36; M	Pulmonary embolism	–	–	A101-O01	A1
17	TG (L + R)	81; F	Cardiac cause	+	+	A101-B101	A1B
18	TG DRG	44; M	Aspiration	+ +	+ +	A101-O01	A1
19	TG (L + R) DRG	63; F	Trauma	– –	– –	O01-O01	O
20	TG	43; M	Trauma	–	–	B101-O01	B
21	TG (L + R)	44; M	Cardiac cause	+	+/–	A101-O01	A1
22	TG (L + R)	81; n.a.	Bleeding from shunt	+	+	A101-O01	A1
23	TG	48; F	Cardiac cause	–	–	O01-O01	O
24	TG	80; F	Trauma	+	+	A101-O01	A1
25	TG (L + R)	78; M	Cardiac cause	–	–	B101-O01	B
26	DRG	60; F	Cardiac cause	–	–	O01-O01	O
27	DRG	61; M	Trauma	–	–	O02-O02	O
28	DRG (n=2)	17; M	Trauma	+	–	A101-O01	A1
29	DRG	26; M	Trauma	+	–	A101-O01	A1
30	DRG (n=2)	43; F	Trauma	–	–	O01-O01	O

TG (L) left trigeminal ganglion, *TG (R)* right trigeminal ganglion, *DRG* dorsal root ganglion, *F* female; *M* male, *n.a.* info not available

informed consent for brain autopsy and the use of the material and clinical information for research purposes had been obtained. The cause of death of the donors analyzed was mainly due to trauma or neurodegenerative diseases but not related to herpesvirus infections. Ganglia were embedded directly in Tissue Tek compound (Sakura, Zoeterwoude, The Netherlands) and stored at −80 °C for subsequent in situ analyses.

The human skin melanoma cell line MeWo was grown to confluent monolayers on coverslips and infected with the VZV strain pOka. At 24 h post-infection, the cells were fixed with acetone and used for immunocytology.

In situ analyses

IHC stainings were performed using predefined optimal dilutions of the following primary antibodies: mouse anti-VZV IE62 (clone MAB8616; Millipore, Schwalbach, Germany) at a dilution of 1:50–1:100, mouse anti-VZV IE63 (clone 9D12; a generous gift of Sebastien Bontems and Catherine Sadzot-Delvaux, Liège, Belgium) (Kennedy et al. 2001) at a dilution of 1:500, and mouse anti-VZV gE (clone MAB8612; Millipore) at a dilution of 1:200 using previously described protocols (Theil et al. 2003; Verjans et al. 2007). Additionally, hybridoma supernatant-derived

IgG1 and IgG2a isotype control mAbs (R&D Systems, Abingdon, UK) were used. In brief, frozen tissue sections were cut, dried, fixed, and endogenous-peroxidase-blocked for 10 min using 1.5–3 % H_2O_2 in methanol, and then incubated with 5–10 % normal rabbit or goat serum followed by incubation with the primary antibody. Primary antibody reactivity was visualized using the avidin–biotin system (DakoCytomation, Heverlee, Belgium) in combination with the substrates 3-amino-9-ethylcarbazole (AEC) or 3,3′-diaminobenzidine (both from Sigma-Aldrich, Deisenhofen, Germany). Finally, the tissue sections were counterstained with hematoxylin (Sigma-Aldrich). Acetone-fixed, VZV-infected MeWo cells were also stained using this protocol, without counterstaining. In case of immunofluorescence (IF) staining, sections were incubated with secondary goat anti-mouse Ig Alexa Fluor 594 (1:500; Invitrogen, Breda, The Netherlands) and mounted in Prolong Gold Antifade Reagent with 4′,6-diamidino-2-phenylindole (DAPI) (Invitrogen).

All stainings were performed in duplicate or triplicate. For quantification, between 100 and 700 neurons per stained tissue section were assessed by two independent researchers. IHC-stained tissue sections were assessed and imaged on an Olympus BX41 microscope (Olympus Europa Holding, Hamburg, Germany) with an Olympus C-4040 Zoom camera. Images were made at ×400 magnification with an air objective. The IF stainings were analyzed on a Zeiss LSM 700 confocal laser scanning microscope (Zeiss, Sliedrecht, The Netherlands). Z-stacks were generated by scanning 21 slices of 0.35 μm thick at 1,112×1,112 pixels, with a Plan-Apochromat ×40/1.3 Oil DIC M27 objective, ×2.5 digital zoom, ×8 frame averaging, and the pinhole adjusted to 1 airy unit. ZEN 2010 software (Zeiss) was used to adjust brightness and contrast and to generate the 3D reconstruction.

The anti-VZV IE62 (MAB8616) and anti-VZV gE (MAB8612) mAbs were adsorbed against human blood group A1 erythrocytes as described (Gorzynski et al. 1964; Wolf et al. 1986; Zerboni et al. 2012). In brief, peripheral blood was extracted in EDTA and centrifuged to pellet the erythrocytes, which were then washed several times with physiological saline. Approximately 500 μl packed erythrocytes were incubated with PBS-diluted antibody. After 1 h at 37 °C, the erythrocytes were centrifuged, and the respective supernatant was used for IHC as described (Gorzynski et al. 1964; Wolf et al. 1986; Zerboni et al. 2012).

ABO genotyping

The ABO blood group genotype of the TG and DRG donors studied was defined by determining the allelic variations in exons 6 and 7 of the donors' ABO gene (Gassner et al. 1996). DNA was extracted from tissue using the Qiagen DNA extraction kit (Qiagen, Valencia, CA, USA). Exons 6 and 7 from the ABO gene were amplified using the high-fidelity DNA polymerase pfuUltra (Stratagene, Amsterdam, The Netherlands) and primers Ex6-F, Ex6-R, Ex7-F1, and Ex7-F2 described in Table 2. Amplification conditions included denaturation for 2 min at 95 °C, followed by 40 cycles 30 s 95 °C, 30 s 57 °C, 1 min at 72 °C, and a final elongation of 3 min at 72 °C. The resulting amplicons were purified from agarose gel using the gel extraction kit from Qiagen and sequenced on the ABIprism 3130XL genetic analyzer with the BigDye Terminator v.1 cycle sequence kit using the above-mentioned primers and the additional internal primers Ex7-F2 and Ex7-R2 (Table 2) for exon 7. The ABO genotype and resultant phenotype of the donor was defined on ABO allele/specific nucleotide alterations within exon 6 (nucleotide positions 261 and 297) and exon 7 (nucleotide positions 467, 526, 646, 657, 681, 703, 796, 802, 803, 829, 930, and 1,059) of the ABO gene (Gassner et al. 1996; Watanabe et al. 2011).

Table 2 Primers used for PCR and sequencing of ABO gene exons 6 and 7

Primer	Sequence	Location[a]	Amplicon size (bp)	Reference
PCR + sequencing				
Ex6-F	5′-AGCTCAGCTTGCTGTGTGTT-3′	Exon 6	528	Watanabe et al. 2011
Ex6-R	5′-AGATGCTGCATGAATGACC-3′	Exon 6		Watanabe et al. 2011
Ex7-F1	5′-GCCTGCCTTGCAGATACGTG-3′	Exon 7	1061[b]	Watanabe et al. 2011
Ex7-R1	5′-TATCTGCGATTGCGTGTCTG-3′	3′-UTR exon 7[c]		
Sequencing				
Ex7-F2	5′-AGGTGGATTACCTGGTGTGC-3′	Exon 7	Not applicable	
Ex7-R2	5′-GTAGAAATCGCCCTCGTCCT-3′	Exon 7	Not applicable	

[a] Location within the ABO gene

[b] The PCR product size is 1,060 bp for A*201 alleles, which have a deletion at position 1,060 in exon 7

[c] 3′-Untranslated region (UTR) of exon 7

Statistical analyses

Data handling, analysis, and graphical representations were performed by using GraphPad Prism 4 software (GraphPad, San Diego, CA). All results are given as mean±SEM. Statistical differences were determined by the paired *t* and chi-square tests. *P* values <0.05 were considered significant.

Results

Intra-neuronal expression of VZV IE62 and IE63 in snap-frozen human TG and DRG

Thirty TG and nine DRG were stained with mAb against the described latency-associated VZV proteins IE62 (clone MAB8616) and IE63 (clone 9D12) (Fig. 1a, b). For both TG and DRG, more ganglia and neurons stained positive with the IE62 mAb compared with IE63. Fourteen of 30 (47 %) TG and four of nine (44 %) DRG were IE62 mAb-positive, whereas only 11 of 30 (37 %) TG and one of nine (11 %) DRG stained positive with the IE63 mAb (Table 1). In TG, the frequency of IE62 mAb-reactive neurons was significantly higher compared with IE63 (17.6 %±2.6 vs 3.8 %±1.3; p=0.0006). An equivalent frequency pattern was observed in the DRG (Fig. 1c). Whereas six of 39 (15 %) ganglia were only IE62 mAb-positive, none of the ganglia stained solely with the IE63 mAb (Table 1). When analyzing serial sections, we observed that IE63 mAb-reactive neurons always co-stained with the IE62 mAb, but not vice versa (Fig. 1a, d). None of the ganglia stained positive with the appropriate isotype control mAb, which were derived from supernatant of in vitro cultured hybridoma cells (data not shown).

We determined the spatial distribution of the IE62 and IE63 mAb signal within individual neurons by laser scanning microscopy. This revealed that the observed signal was localized in vesicular-like structures throughout the cytoplasm (Fig. 2; arrow). These structures were clearly discernible from the intracellular deposits of neuromelanin and lipofuscin that had a more punctuated dense structure and autofluorescent properties (Fig. 2; arrowhead). When Z-stacks were examined in both the *X*- and *Y*-axis orientation, the VZV mAb-reactive vesicles were partially interconnected within the cytoplasm of VZV latently infected human TG neurons (Fig. 2; arrowhead).

Donor's blood group A1 status correlates with IE62 and IE63 mAb reactivity

The exclusive cytoplasmic IE62 and IE63 mAb staining pattern in VZV latently infected neurons contrasts with the predominant nuclear localization of both proteins during lytic infection (Lungu et al. 1998). The high frequency of VZV-specific mAb-reactive neurons is also discordant with

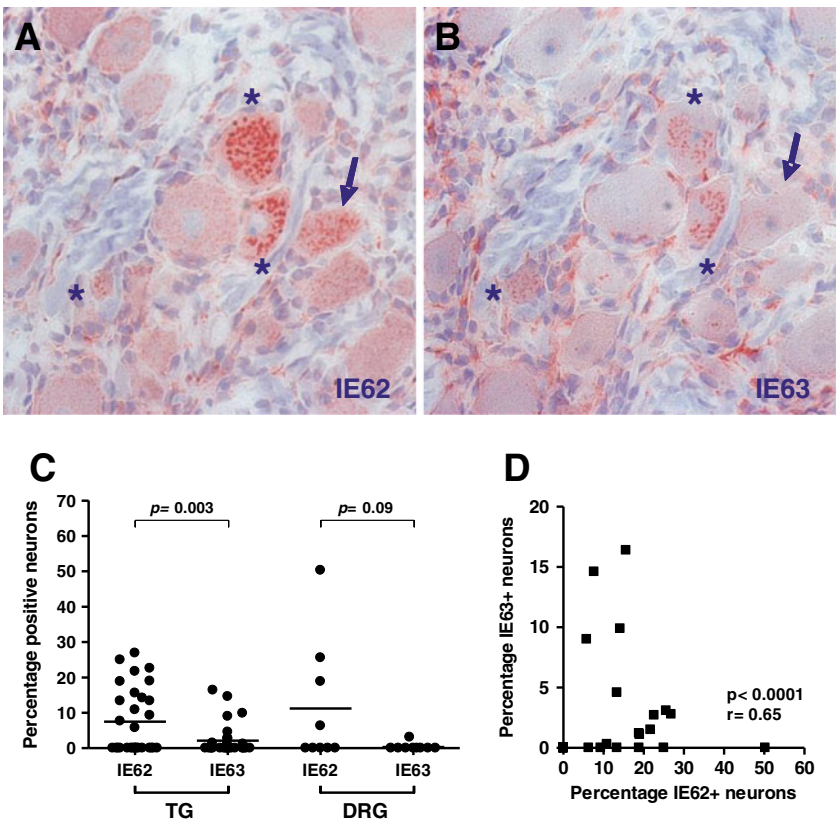

Fig. 1 Immunohistochemistry with anti-VZV IE62 and IE63 mAb on snap-frozen human TG and DRG. **a**, **b** Consecutive human TG sections were stained with anti-IE62 mAb (**a**) and IE63 mAb (**b**). Sections were developed and counter-stained with AEC and hematoxylin resulting in a red color and blue nuclei, respectively. Neurons reactive with both IE62 and IE63 mAbs and those that are single IE62 mAb-positive are indicated by an *asterisk* and *arrow*, respectively. Magnification, ×400. **c** Percentage IE62 and IE63 mAb-positive neurons in TG and DRG. **d** Intra-donor correlation between IE62 and IE63 mAb-positive neurons

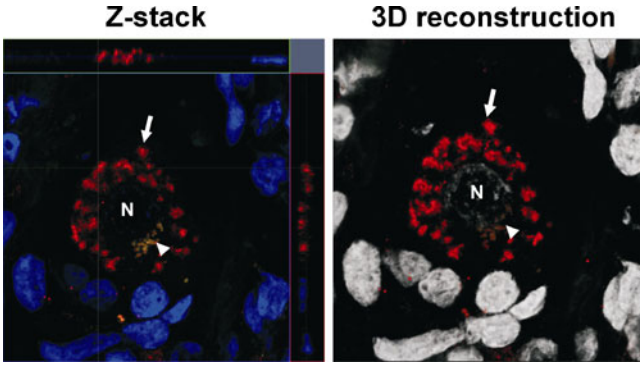

Fig. 2 Intracellular localization of the VZV IE62 mAb signal in human TG neurons. Human TG sections were stained for VZV IE62 (Alexa Fluor 594, *red* color) and nuclei were visualized using DAPI (*blue* and *gray color* in *left* and *right panels*, respectively). The specimen was analyzed in a Zeiss LSM 700 confocal microscope and a Z-stack (21 slices, 0.35 μm thick) of images at ×400 magnification and ×2.5 digital zoom was taken showing one VZV IE62 mAb-positive TG neuron. *Left panel* shows slice 12 from the Z-stack with the smaller side panels showing the view from X and Y. Note that in the X and Y view the IE62 mAb-positive vesicles appear to be interconnected. *Right panel* shows a 3D reconstruction of the Z-stack, demonstrating that the IE62 mAb signal is located in vesicular-like structures that seem to be interconnected and are spread throughout the neuronal cytoplasm, consistent with the golgi compartment. *Long arrows* indicate VZV IE62 mAb staining and *arrow heads* indicate lipofuscin. *N*, nucleus

the expected frequency of only 1 % to 6.9 % VZV DNA containing neurons in VZV latently infected neurons (Wang et al. 2005).

Recently, Zerboni and colleagues have shown that the IHC signal is most likely the result of a mouse ascites Golgi (MAG) reaction to human blood group A1-associated antigens. The formalin fixation in that study may, however, have selectively released the MAG-specific epitopes. To ascertain the causal role of the donor's blood type to staining frequency and pattern, the blood group of the 30 donors under investigation was determined by sequencing exons 6 and 7 of the ABO blood group gene (Watanabe et al. 2011). Seventeen donors had an A1 phenotype, consisting of donors with the following phenotypes A1;A2 (n=3), A1;B (n=3), and A1 (n=11) (Table 1). Whereas none of the $A1^{NEG}$ donors had IE62 and IE63 mAb-positive neurons, a significant correlation between the donor's A1 phenotype and IE62 ($p<0.0001$) and IE63 ($p=0.003$) mAb staining was detected. The frequency of VZV mAb-positive neurons was not different between $A1^{POS}$ donors with different A1 genotypes. Among the 22 ganglia from $A1^{POS}$ donors, 12 of 22 (55 %) stained positive with both mAbs and six of 22 (27 %) were solely IE62 mAb-positive. Notably, four of 22 (18 %) ganglia from $A1^{POS}$ donors did not stain with either anti-VZV mAb (Table 1).

To consolidate that the observed anti-VZV mAb IHC signal was due to endogenous contaminating antibodies directed against blood group A1-associated antigens, anti-IE62 and glycoprotein E ascites-derived mAb preparations were adsorbed against blood group A1 erythrocytes. Whereas both the original and adsorbed mAbs stained VZV-infected cells without discernable differences (Fig. 3), intra-neuronal mAb reactivity was completely eliminated upon adsorption by A1 erythrocytes (Fig. 3).

Discussion

Elucidation of the virus and host factors involved during VZV latency in sensory ganglia is vital to optimize existing treatments and to develop new therapeutic intervention strategies to prevent recrudescent VZV infections. The application of VZV ORF multiplex RT-PCR, and more recently GeXPS technology covering the whole VZV transcriptome, has provided a comprehensive overview of the VZV transcripts expressed during latency (reviewed in: Kennedy and Cohrs 2010). Contrastingly, due to the limited availability of anti-VZV antibodies for in situ analysis, our knowledge of the VZV latency-associated proteome is far from complete.

The expression of the VZV proteins IE62 and IE63 has been studied extensively in latently infected human sensory ganglia since they are considered as the prototypic latency-associated VZV proteins (Cohrs and Gilden 2003; Grinfeld and Kennedy 2004; Kennedy et al. 2000; Lungu et al. 1998; Mahalingam et al. 1996; Theil et al. 2003; Zerboni et al. 2010). Several groups have reported on the intra-neuronal expression of both proteins in human DRG and TG but with discordant results on the number of ganglia positive and the frequency of protein expressing neurons per ganglion. IE62 has been detected in 6–10 % of neurons of all DRG tested using mouse ascites mAb and polyclonal rabbit antibodies (Lungu et al. 1998), with 5–10 % of neurons positive in all tested TG using a polyclonal antibody (Grinfeld and Kennedy 2004) and with 2.5–8 % of neurons positive in eight of 21 TG analyzed using the same mouse IE62 antibody used in the present study (Theil et al. 2003). For IE63, the varying detection frequencies between laboratories are also significant and can be related to the antibodies used: Very rare neurons in five of 21 ganglia (Mahalingam et al. 1996) and five of 20 TG (Kennedy et al. 2000) were found to be IE63-positive using the same polyclonal rabbit antibody, while using a different rabbit anti-IE63 antibody also gave few positive neurons in only one of 27 tested ganglia (Zerboni et al. 2010). Other studies, however, show a more abundant apparent VZV protein expression, with 3–9 % of neurons from all DRG positive using a polyclonal rabbit antibody (Lungu et al. 1998), whilst using a mouse monoclonal antibody from ascites in TG from ten subjects stained 5 % to 10 % of neurons as positive (Grinfeld and Kennedy 2004; Kennedy et al. 2001). Herein, we used the same IE62 and

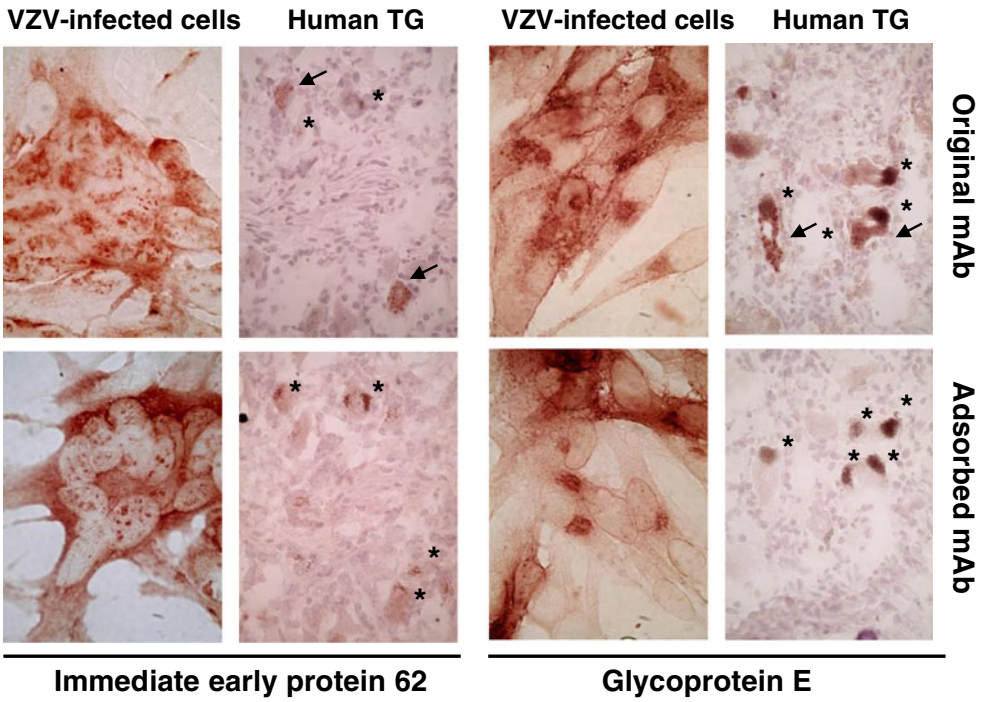

Fig. 3 Abrogation of neuronal VZV mAb reactivity in snap-frozen TG and DRG upon adsorption by blood group A1 erythrocytes. Mouse monoclonal ascites-derived VZV IE62- and glycoprotein E-specific mAbs were adsorbed against blood group A1 erythrocytes or left untreated. Both non-adsorbed (*top row panels*) and adsorbed (*bottom row panels*) anti-VZV mAbs equally reacted with their respective antigens in VZV-infected MeWo cells. In contrast, intra-neuronal immunoreactivity of both mAbs in snap-frozen human TG was completely abrogated by adsorption with blood group A1 erythrocytes

IE63 mAb to detect the respective VZV proteins in snap-frozen human TG and DRG and found a high number of positive ganglia with relatively high frequencies of mAb-reactive neurons. Notably, IE63 mAb reactivity correlated with IE62, suggesting an interaction between both stainings (Table 1 and Fig. 1).

One important cause for the aforementioned discordant IE62 and IE63 IHC results was recently highlighted in a study by Zerboni and colleagues (Zerboni et al. 2012). They demonstrated that VZV-specific ascites-derived mouse mAb and rabbit polyclonal antibodies contain endogenous contaminating antibodies reacting with blood group A1-associated antigens in formalin-fixed and paraffin-embedded human DRG. The present study on human snap-frozen DRG and TG supports this concept. First, the intra-neuronal IE62 and IE63 mAb reactivity correlated significantly with the TG/DRG donor's blood group A1 genotype status, and second, the IHC staining was abolished by adsorption of VZV mAb against blood group A1 erythrocytes (Table 1 and Fig. 3). There was no correlation between the frequency of neuronal staining and post-mortem delay, suggesting that neither this variable nor the fixation method is important for the availability of blood group A1-associated antigens.

Staining of particular tissues and cells from blood group $A1^{POS}$ donors with mouse ascites-derived mAb is due to the so-called MAG reaction. The MAG epitopes are considered blood group A1 oligosaccharides (Kliman et al. 1995), which are also expressed by sensory neurons within Golgi-associated vacuoles that closely resemble the VZV mAb-positive vesicular structures shown in Fig. 2 (Dodd and Jessell 1985; Mollicone et al. 1986). The expression of the MAG epitopes varies between ganglia (e.g., cervical vs thoracic) and is limited to certain sub-classes of neurons (Mollicone et al. 1986). In the present study, we found differences in IE62 and IE63 mAb reactivity between ganglia from the same individual, as well as differences in the percentage of neurons positively stained with each mAb over the studied population. The limited expression of the MAG epitopes in only certain ganglion and neuron types could explain such varying anti-VZV antibody staining frequencies described previously and those reported here. Alternatively, different antibody preparations may contain variable concentrations of MAG-reactive antibodies. Furthermore, despite using multiple lots of VZV IE62-specific antibodies, we did not observe differences in antibody reactivity within and between donors using different antibody batches (data not shown).

In conclusion, the data presented here consolidate the previous report by Zerboni and colleagues (Zerboni et al. 2012) and extend the MAG reaction of ascites-derived anti-VZV mAbs to snap-frozen human sensory ganglion tissues. As a synthesis of both studies, it emerges that ascites-derived mAb preparations should be screened for reactivity against blood group A1-associated antigens to avoid misinterpretation of intra-cellular detection of virus and host proteins in both formalin-fixed and snap-frozen human ganglia. The described blood group A1 erythrocyte adsorption procedure allows depletion of the MAG-reactive contaminating antibodies from ascites-derived mAb preparations to circumvent aberrant IHC staining patterns in the future. The MAG reaction is not restricted to sensory ganglia or anti-

viral antibodies, as highlighted by several other publications on this phenomenon (Finstad et al. 1991; Kliman et al. 1995). The extent of VZV translation during latency remains an important issue that will require careful re-evaluation using both current IHC methods and new tools.

Acknowledgments The authors thank Sebastien Bontems and Catherine Sadzot-Delvaux (Liège, Belgium) for the generous gift of the VZV IE63 mAb; Susanne Bailer (Munich, Germany) for providing the VZV-infected MeWo cells; and Freek van Loenen (Rotterdam, The Netherlands) for technical assistance with the ABO blood group genotyping. This study was supported by a grant from the BMBF (German Ministry for Education and Research) IFB-01EO0901 to K.H.

References

Arvin AM (1996) Varicella-zoster virus. Clin Microbiol Rev 9:361–381

Cohrs RJ, Gilden DH (2003) Varicella zoster virus transcription in latently-infected human ganglia. Anticancer Res 23:2063–2069

Cohrs RJ, Gilden DH (2007) Prevalence and abundance of latently transcribed varicella-zoster virus genes in human ganglia. J Virol 81:2950–2956

Cohrs RJ, Srock K, Barbour MB, Owens G, Mahalingam R, Devlin ME, Wellish M, Gilden DH (1994) Varicella-zoster virus (VZV) transcription during latency in human ganglia: construction of a cDNA library from latently infected human trigeminal ganglia and detection of a VZV transcript. J Virol 68:7900–7908

Cohrs RJ, Barbour M, Gilden DH (1996) Varicella-zoster virus (VZV) transcription during latency in human ganglia: detection of transcripts mapping to genes 21, 29, 62, and 63 in a cDNA library enriched for VZV RNA. J Virol 70:2789–2796

Cohrs RJ, Gilden DH, Kinchington PR, Grinfeld E, Kennedy PG (2003) Varicella-zoster virus gene 66 transcription and translation in latently infected human ganglia. J Virol 77:6660–6665

Croen KD, Ostrove JM, Dragovic LJ, Smialek JE, Straus SE (1987) Latent herpes simplex virus in human trigeminal ganglia. Detection of an immediate early gene "anti-sense" transcript by in situ hybridization. N Engl J Med 317:1427–1432

Dodd J, Jessell TM (1985) Lactoseries carbohydrates specify subsets of dorsal root ganglion neurons projecting to the superficial dorsal horn of rat spinal cord. J Neurosci 5:3278–3294

Finstad CL, Yin BW, Gordon CM, Federici MG, Welt S, Lloyd KO (1991) Some monoclonal antibody reagents (C219 and JSB-1) to P-glycoprotein contain antibodies to blood group A carbohydrate determinants: a problem of quality control for immunohistochemical analysis. J Histochem Cytochem 39:1603–1610

Gassner C, Schmarda A, Nussbaumer W, Schonitzer D (1996) ABO glycosyltransferase genotyping by polymerase chain reaction using sequence-specific primers. Blood 88:1852–1856

Gorzynski EA, Brodhage H, Neter E (1964) Hemagglutination by mixtures of enterobacterial antigen and *Shigella sonnei* antiserum. Z Hyg Infektionskr 150:1–9

Grinfeld E, Kennedy PG (2004) Translation of varicella-zoster virus genes during human ganglionic latency. Virus Genes 29:317–319

Inoue H, Motani-Saitoh H, Sakurada K, Ikegaya H, Yajima D, Hayakawa M, Sato Y, Otsuka K, Kobayashi K, Nagasawa S, Iwase H (2010) Detection of varicella-zoster virus DNA in 414 human trigeminal ganglia from cadavers by the polymerase chain reaction: a comparison of the detection rate of varicella-zoster virus and herpes simplex virus type 1. J Med Virol 82:345–349

Kennedy PG, Cohrs RJ (2010) Varicella-zoster virus human ganglionic latency: a current summary. J Neurovirol 16:411–418

Kennedy PG, Grinfeld E, Gow JW (1999) Latent varicella-zoster virus in human dorsal root ganglia. Virology 258:451–454

Kennedy PG, Grinfeld E, Bell JE (2000) Varicella-zoster virus gene expression in latently infected and explanted human ganglia. J Virol 74:11893–11898

Kennedy PG, Grinfeld E, Bontems S, Sadzot-Delvaux C (2001) Varicella-zoster virus gene expression in latently infected rat dorsal root ganglia. Virology 289:218–223

Kliman HJ, Feinberg RF, Schwartz LB, Feinman MA, Lavi E, Meaddough EL (1995) A mucin-like glycoprotein identified by MAG (mouse ascites golgi) antibodies. Menstrual cycle-dependent localization in human endometrium. Am J Pathol 146:166–181

Lungu O, Panagiotidis CA, Annunziato PW, Gershon AA, Silverstein SJ (1998) Aberrant intracellular localization of varicella-zoster virus regulatory proteins during latency. Proc Natl Acad Sci USA 95:7080–7085

Mahalingam R, Wellish MC, Dueland AN, Cohrs RJ, Gilden DH (1992) Localization of herpes simplex virus and varicella zoster virus DNA in human ganglia. Ann Neurol 31:444–448

Mahalingam R, Wellish M, Cohrs R, Debrus S, Piette J, Rentier B, Gilden DH (1996) Expression of protein encoded by varicella-zoster virus open reading frame 63 in latently infected human ganglionic neurons. Proc Natl Acad Sci USA 93:2122–2124

Meier JL, Holman RP, Croen KD, Smialek JE, Straus SE (1993) Varicella-zoster virus transcription in human trigeminal ganglia. Virology 193:193–200

Mick G (2010) Vaccination: a new option to reduce the burden of herpes zoster. Expert Rev Vaccines 9:31–35

Mollicone R, Davies DR, Evans B, Dalix AM, Oriol R (1986) Cellular expression and genetic control of ABH antigens in primary sensory neurons of marmoset, baboon and man. J Neuroimmunol 10:255–269

Nagel MA, Choe A, Traktinskiy I, Cordery-Cotter R, Gilden D, Cohrs RJ (2011) Varicella-zoster virus transcriptome in latently infected human ganglia. J Virol 85:2276–2287

Oxman MN, Levin MJ, Johnson GR, Schmader KE, Straus SE, Gelb LD, Arbeit RD, Simberkoff MS, Gershon AA, Davis LE, Weinberg A, Boardman KD, Williams HM, Zhang JH, Peduzzi PN, Beisel CE, Morrison VA, Guatelli JC, Brooks PA, Kauffman CA, Pachucki CT, Neuzil KM, Betts RF, Wright PF, Griffin MR, Brunell P, Soto NE, Marques AR, Keay SK, Goodman RP, Cotton DJ, Gnann JW Jr, Loutit J, Holodniy M, Keitel WA, Crawford GE, Yeh SS, Lobo Z, Toney JF, Greenberg RN, Keller PM, Harbecke R, Hayward AR, Irwin MR, Kyriakides TC, Chan CY, Chan IS, Wang WW, Annunziato PW, Silber JL (2005) A vaccine to prevent herpes zoster and postherpetic neuralgia in older adults. N Engl J Med 352:2271–2284

Stevens JG, Wagner EK, vi-Rao GB, Cook ML, Feldman LT (1987) RNA complementary to a herpesvirus alpha gene mRNA is prominent in latently infected neurons. Science 235:1056–1059

Theil D, Derfuss T, Paripovic I, Herberger S, Meinl E, Schueler O, Strupp M, Arbusow V, Brandt T (2003) Latent herpesvirus infection in human trigeminal ganglia causes chronic immune response. Am J Pathol 163:2179–2184

Verjans GM, Hintzen RQ, van Dun JM, Poot A, Milikan JC, Laman JD, Langerak AW, Kinchington PR, Osterhaus AD (2007) Selective retention of herpes simplex virus-specific T cells in latently infected human trigeminal ganglia. Proc Natl Acad Sci USA 104:3496–3501

Wang K, Lau TY, Morales M, Mont EK, Straus SE (2005) Laser-capture microdissection: refining estimates of the quantity and distribution of latent herpes simplex virus 1 and varicella-zoster virus DNA in human trigeminal ganglia at the single-cell level. J Virol 79:14079–14087

Watanabe K, Ikegaya H, Hirayama K, Motani H, Iwase H, Kaneko H, Fukushima H, Akutsu T, Sakurada K (2011) A novel method for ABO genotyping using a DNA chip. J Forensic Sci 56(Suppl 1): S183–S187

Wolf MF, Koerner U, Schumacher K (1986) Specificity of reagents directed to the Thomsen-Friedenreich antigen and their capacity to bind to the surface of human carcinoma cell lines. Cancer Res 46:1779–1782

Zerboni L, Sobel RA, Ramachandran V, Rajamani J, Ruyechan W, Abendroth A, Arvin A (2010) Expression of varicella-zoster virus immediate-early regulatory protein IE63 in neurons of latently infected human sensory ganglia. J Virol 84:3421–3430

Zerboni L, Sobel RA, Lai M, Triglia R, Steain M, Abendroth A, Arvin A (2012) Apparent expression of varicella-zoster virus proteins in latency resulting from reactivity of murine and rabbit antibodies with human blood group A determinants in sensory neurons. J Virol 86:578–583